Marchenko redatuming: advantages and limitations in complex media

Ivan Vasconcelos, Schlumberger Gould Research, Dirk-Jan van Manen, ETH Zurich, Matteo Ravasi, University of Edinburgh, Kees Wapenaar and Joost van der Neut, Delft University of Technology.*

Summary

The novel technique of Marchenko redatuming can retrieve waves in the subsurface including primaries and multiples. We interpret the Marchenko scheme as an approach to overcome "incomplete time reversal": the method can be thought of as exciting focusing fields from one-sided "secondary sources", that yield subsurface-redatumed waves as if a complete two-sided experiment were available. These secondary focusing fields are retrieved directly from one-sided reflection data by means of an iterative autofocusing scheme. Here, we discuss the key components of the Marchenko scheme and their underlying assumptions, these being: knowledge of the medium's reflection response, and the choice of an initial focusing function and a data separation filter necessary for the iterative procedure. Using a complex subsalt benchmark model, we show that the current implementation of Marchenko redatuming outperforms conventional wavefield extrapolation in estimating the desired subsurface fields. Firstly, the Marchenko method suppresses prominent artifacts that arise in conventional extrapolation during the iterative scheme. More importantly, we observe that Marchenko redatuming succeeds in estimating a downgoing transmitted field containing internal multiples that cannot be obtained by conventional extrapolation using the same model. We discuss the assumptions of the current Marchenko scheme, suggesting directions for improving the scheme to handle highly complex media such as subsalt.

Introduction

The retrieval of wavefields within the earth's subsurface where no receivers or sources are available is a key component of wave-equation imaging and inversion, and yet retrieving full wave responses containing internal multiples with correct amplitudes has long presented a challenge to imaging practice. Recently, the method of Marchenko redatuming or autofocusing (Broggini et al., 2011; Wapenaar et al., 2013a) proposes to retrieve wave responses inside the subsurface, with correct amplitudes and internal multiples, using relatively little information about the earth's properties. Although still in development, the fields retrieved Marchenko redatuming can in principle be used to improve imaging beyond current capabilities, as discussed by Behura et al. (2012), van der Neut et al. (2013), Vasconcelos and Rickett (2013), Broggini et al. (2014), Ravasi et al. (2014) and Vasconcelos et al. (2014). While indeed capable of retrieving internal multiples and correcting amplitudes, recent studies in the presence of strongly scattering media brought forth some limitations of the current practical implementation of the Marchenko scheme (van der Neut et al., 2014; Wapenaar et al., 2014). With the aim of using Marchenko in geologically complex media, we build on the physical interpretation of the Marchenko scheme, review its key components and assumptions, and analyse the performance of the current practical implementation in a complex subsalt model.

Incomplete time reversal and one-sided focusing

We begin by considering a series of thought experiments in time reversal as illustrated by Figure 1. We consider the case where the medium is completely bounded by receivers (Figure 1a) or only bounded on one side of the medium (Figure 1b). In either of these cases, we assume that time reversal can be done by "exact injection" of the boundary fields (van Manen et al., 2007) in the real medium, so there are no errors associated with the wavefield injection process. In the ideal time-reversal scenario in Figure 1a, all constructively-interfering waves propagate backward from the receivers through the same physical paths that are sampled in the forward-time experiment, providing a perfectly focused field at the source location. On the other hand, if time-reversal is conducted from receivers on one side of the medium (Figure 1b), only some of the backprogating waves travel through the correct paths and focus at the source location (solid black arrows), while at the same time creating spurious waves (dotted red arrows) from their interactions with the medium discontinuities. In the case of Figure 1b, time reversal is incomplete and thus the fields do not focus perfectly at the source location only.

As an alternative to having the bottom boundary of receivers in Figure 1a for time reversal, let us say that we want to achieve a time-reversed field that focuses properly only at the desired location but having receivers on only one side of the medium as in Figure 1b. We refer to this as one-sided focusing. It is clear from the picture in Figure 1b that something must be done in addition to conventional time-reversal to account for the spurious arrivals and to reconstruct physical wavepaths associated to the missing boundary. To do this, we introduce the concept of using "secondary sources" that excite waves on the top boundary and produce a "focusing field" in the subsurface: these sources (red stars in Figure 1c) both replace and complement the original one-sided time-reversed fields. This one-sided secondary source field is fit-for-purpose: it is designed to precisely cancel spurious events (solid red arrows), while at the same time retrieving waves that correspond to the missing physical arrivals at the focusing source location (dotted black arrows). If such a field could be constructed, then one-sided focusing in the context of Figure 1c would perhaps yield an acceptable estimate of field focused at the desired location in a complete time reversal experiment (Figure 1a).

Redatuming by Marchenko autofocusing

One-sided focusing as illustrated by Figure 1c is the goal of the redatuming methods presented by Broggini et al. (2012) and Wapenaar et al. (2013a). These methods are based on the so-called Marchenko integral equations (Wapenaar et al., 2013b):

$$\hat{p}^-(\mathbf{x}_a,\mathbf{x}_r) = \int_{\partial\mathbb{D}_0} \hat{R}(\mathbf{x}_r,\mathbf{x}_s)\,\hat{f}_1^+(\mathbf{x}_s,\mathbf{x}_a)\,d\mathbf{x}_s - \hat{f}_1^-(\mathbf{x}_r,\mathbf{x}_a)\,, \quad (1)$$

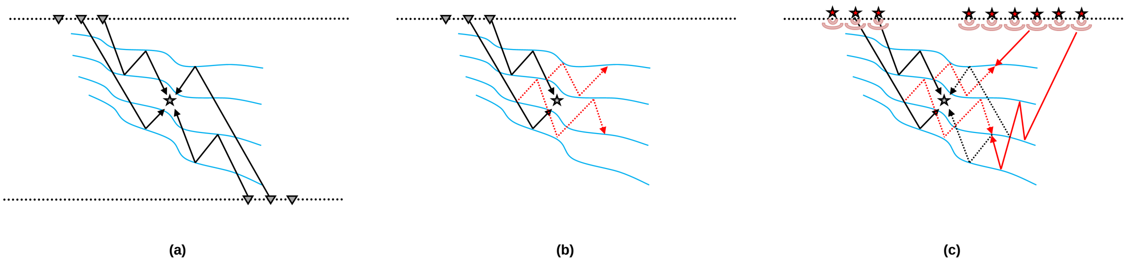

Figure 1: Illustrations of time reversal of fields originally excited by a source in the medium (grey star) and recorded by boundary receivers (grey triangles). Panel (a) depicts a complete time reversal scenario. In panel (b), the boundary data are only available on one side of the medium, leading to an incomplete time reversal containing both physical waves (black arrows) and unphysical arrivals (dotted red arrows). In panel (c), the incomplete time reversal experiment is replaced by one-sided secondary sources (denoted by the red stars), designed to cancel the unphysical waves in (b) as denoted by dotted red arrows, while simultaneously reconstructing physical wavepaths (black arrows) that focus at the desired source location as in panel (a).

and

$$\hat{p}^{+}(\mathbf{x}_a,\mathbf{x}_r) = -\int_{\partial\mathbb{D}_0} \hat{R}(\mathbf{x}_r,\mathbf{x}_s)\,\left\{\hat{f}_1^{-}(\mathbf{x}_s,\mathbf{x}_a)\right\}^{*} d\mathbf{x}_s + \left\{\hat{f}_1^{+}(\mathbf{x}_r,\mathbf{x}_a)\right\}^{*}. \quad (2)$$

Here, $\mathbf{x}_s$ and $\mathbf{x}_r$ are source and receiver locations on a boundary $\partial\mathbb{D}_0$ on top of the medium, and $\mathbf{x}_a$ is an arbitrary location in the inside of the medium. The fields $\hat{p}^{-}$ and $\hat{p}^{+}$ are, respectively, the up- and down-going components of the field as if observed by a receiver at $\mathbf{x}_a$, so that $\hat{p} = \hat{p}^{+} + \hat{p}^{-}$ is the total desired field at depth. The broadband reflection response of the medium at the top boundary, $\hat{R}(\mathbf{x}_r,\mathbf{x}_s)$, is assumed to be known. All equations and quantities presented here are in the frequency domain for the sake of notation brevity. As such * denotes complex conjugation, i.e., a time-reversal in the time domain, and the integrals in equations 1 and 2 correspond to multidimensional convolutions in the time domain.

The focusing functions $\hat{f}_1$ deserve special attention, as these are associated to the idea of the secondary sources in Figure 1: these are "injected" into the medium by means of the multidimensional convolution with the one-sided reflection response as seen in equations 1 and 2. More precisely, $\hat{f}_1^{+}$, the down-going component of the focusing function, is defined as an inverse of the real medium's transmission operator via

$$\delta(\mathbf{x}_a - \mathbf{x}'_a) = \int_{\partial\mathbb{D}_0} \hat{T}(\mathbf{x}_a,\mathbf{x})\,\hat{f}_1^{+}(\mathbf{x},\mathbf{x}'_a)\,d\mathbf{x}, \quad (3)$$

where both $\mathbf{x}_a$ and $\mathbf{x}'_a$ are points on an arbitrary subsurface datum $\partial\mathbb{D}_a$, with $\hat{T}(\mathbf{x}_a,\mathbf{x})$ being the full transmission response between $\partial\mathbb{D}_a$ and the top surface $\partial\mathbb{D}_0$. The upgoing focusing field $\hat{f}_1^{-}$, on the other hand, thus implicitly relates the medium's transmission and reflection responses with the desired focusing fields as seen in equations 1 and 2.

The desired fields $\hat{p}^{-}$ and $\hat{p}^{+}$ can be solved for, using the Marchenko system in equations 1 and 2, in two steps. The first step is to iteratively estimate the focusing functions

$$\hat{f}_{1,k}^{-}(\mathbf{x}_r,\mathbf{x}_a) = \hat{S} \overset{\omega}{*} \int_{\partial\mathbb{D}_0} \hat{R}(\mathbf{x}_r,\mathbf{x}_s)\,\left\{\hat{f}_{1,0}^{+}(\mathbf{x}_s,\mathbf{x}_a) + \hat{f}_{M1,k}^{+}(\mathbf{x}_s,\mathbf{x}_a)\right\} d\mathbf{x}_s \quad (4)$$

and

$$\left\{\hat{f}_{M1,k}^{+}(\mathbf{x}_r,\mathbf{x}_a)\right\}^{*} = \hat{S} \overset{\omega}{*} \int_{\partial\mathbb{D}_0} \hat{R}(\mathbf{x}_r,\mathbf{x}_s)\,\left\{\hat{f}_{1,k}^{-}(\mathbf{x}_s,\mathbf{x}_a)\right\}^{*} d\mathbf{x}_s, \quad (5)$$

where the subscript k is the iteration number and $\overset{\omega}{*}$ denotes frequency-domain convolution. The choice of the filter $\hat{S}$ is key: it acts as a separation filter in equations 1 and 2 to isolate the $\hat{f}_1$ functions (see below). The function $\hat{f}_{1,0}^{+}$ is a first guess estimate of $\hat{f}_1^{+}$, and the initial $\hat{f}_{1,0}^{-} = 0$. Note that $\hat{f}_{1,k}^{+} = \hat{f}_{1,0}^{+} + \hat{f}_{M1,k}^{+}$, with the update $\hat{f}_{M1,k}^{+}$ being a "coda" of $\hat{f}_{1,k}^{+}$. Once this iterative step is complete, we assign $\hat{f}_1^{\pm} = \hat{f}_{1,k}^{\pm}$, and use these estimated fields, together with the known reflection response, to obtain the desired redatumed fields $\hat{p}^{-}$ and $\hat{p}^{+}$ once again using equations 1 and 2.

This brings us to the three key components of the Marchenko redatuming scheme:

1. Knowledge of $\hat{R}(\mathbf{x}_r,\mathbf{x}_s)$. If reflection data are taken as a proxy for the real medium's reflection response, the method assumes large-aperture, fixed-spread receiver arrays with dense source coverage over the entire spread. Moreover, $\hat{R}$ is of infinite bandwidth and dimensionless, so reflection data are assumed to be deconvolved of source and receiver effects, and properly scaled relative to $\hat{f}_{1,0}^{+}$.
2. Choice of $\hat{f}_{1,0}^{+}$. As equation 3 shows, $\hat{f}_1^{+}$ is an inverse of the true medium's transmission response. Given an initial guess model of the subsurface, $\hat{f}_{1,0}^{+}$ should be an estimate of the inverse transmission response in that model, however, current practice approximates that estimate using simply $\{\hat{p}_0^{+}\}^{*}$, with $\hat{p}_0^{+}$ being the reference transmission field.
3. Choice of $\hat{S}$. For the iterative focusing step to hold, this filter must ideally satisfy both $\hat{S} \overset{\omega}{*} \hat{p}^{\pm} = 0$, $\hat{S} \overset{\omega}{*} \hat{f}_1^{-} = \hat{f}_1^{-}$ and $\hat{S} \overset{\omega}{*} \hat{f}_1^{+*} = \hat{f}_1^{+*}$. Current practice is based on time-domain windowing of arrivals that do not obey wave causality in the reference model used to estimate $\hat{f}_{1,0}^{+}$ (Wapenaar et al., 2013b).

Below we discuss the effect of these three key components in redatuming, with a focus on components 2 and 3, in the context of highly heterogeneous media (e.g., subsalt).

Subsalt example

For our subsalt example, we use the Sigsbee model in Figure 2. In Figure 2a, we show the “true model” used to generate the reflection data required as input to the Marchenko scheme, as well as to compute the benchmark scattered wavefield response in Figure 3a. Figure 2b shows the reference model used for extrapolation and Marchenko redatuming, representing an industry-standard migration velocity model based on Figure 2a. Modeling is done using a finite-difference vector-acoustic scheme (e.g., Vasconcelos, 2013), with a 20 Hz Ricker wavelet, using densely-sampled sources and receivers as shown in Figure 2. The reflection data are source-wavelet deconvolved to approximate the $R(\mathbf{x}_r, \mathbf{x}_s, t)$ operator required by the Marchenko scheme. We also model the reference transmitted field p_0^+ (Figure 3c) in the reference model in Figure 2b.

As in Wapenaar et al. (2013a), in our implementation of the Marchenko scheme, we use set $f_{1,0}^+(\mathbf{x}_s, \mathbf{x}_a, t) = p_0^+(\mathbf{x}_s, \mathbf{x}_a, -t)$ (Figure 3c) to drive the iterative procedure 4. $S(\mathbf{x}_s, \mathbf{x}_a, t)$ is chosen as a time-domain mask that only preserves energy in the interval $-t_w < t < t_w$. Here, $t_w(\mathbf{x}_s, \mathbf{x}_a) = t_d(\mathbf{x}_s, \mathbf{x}_a) - \varepsilon$, where $t_d(\mathbf{x}_s, \mathbf{x}_a)$ is the direct-wave traveltime computed with a fast-marching eikonal solver, and ε is chosen as a fraction of the dominant period. After three iterations of equations 4 and 5, we obtain the fields in Figure 4, noting here that the scattered fields $p_S^{-,+} = p^{-,+} - p_0^+$, i.e., the fields in Figure 4a and 4b are the ones in equations 1 and 2 minus the modeled reference field in Figure 3c. Given that the full field in the true model is $p^{true} = p_S^{true} + p_0^+$, separating the scattering components allows us to identify what is really retrieved by the Marchenko scheme in light of the complexity of the reference field in Figure 3c. The field in Figure 3b is the total Marchenko-redatumed field, i.e., the superposition of the down- and upgoing components in Figures 4a and 4b.

Inspection of the redatuming results in Figure 3 reveals that the current Marchenko scheme retrieves a substantially better estimate of the true scattered field in the subsurface than that obtained by conventional reverse-time extrapolation. This is an important result noting that both Marchenko redatuming and conventional reverse-time extrapolation use the same model in Figure 2b. Comparing the redatumed fields in Figure 4 with those in Figure 3, we see that the p_S^- field retrieves the upgoing waves present in conventional extrapolation, but with different amplitudes and without the prominent artifacts in the p_0^- field that occur before the first arrivals in p_0^+. These artifacts are in fact used by the Marchenko scheme, as it can be seen in the f_1^- field. More importantly, we note that some of the most prominent features of the Marchenko-retrieved p_S^{auto} field in Figure 3 belong to the reconstructed downgoing transmitted field p_S^+: Marchenko redatuming provides non-neglible amplitude corrections and reconstructs downgoing internal multiples that cannot be obtained using the known model, i.e., that are not present in the p_0^+ field.

Although Marchenko redatuming clearly outperforms conventional wavefield extrapolation in this complex subsalt example, close comparison of the retrieved p_S^{auto} with p_S^{true} shows that the current implementation of the Marchenko scheme does retrieve many of the arrivals, but it also misses several others. Furthermore, the reconstruction of the first-arrival transmitted amplitudes is not as accurate as in previous examples such as by Broggini et al. (2012) and Wapenaar et al. (2013a). We attribute these inaccuracies to the current assumptions underlying the initial $f_{1,0}^+$ as a simple time-reversal of a reference field, and the filter M being defined as masking in the time domain. While these choices provide good approximations for the key components of Marchenko redatuming in simpler models (Broggini et al., 2012; Wapenaar et al., 2013a), they become less suitable choices in the presence of lateral heterogeneity and scattering (van der Neut et al., 2014). Better choices of $f_{1,0}^+$ and S to account for more general media and improve Marchenko redatuming in environments such as subsalt are subject of ongoing research.

Conclusions

In this study, we push the limits of Marchenko redatuming by applying it to a highly complex subsalt benchmark model. In our experiments, both Marchenko redatuming and conventional reverse-time extrapolation rely on the same industry-standard migration velocity model. Despite using the same model, our results show that Marchenko redatuming provides a considerably better estimate of the true subsurface fields. This is true for the upgoing subsurface field where the iterative muting eliminates prominent artifacts present in conventional extrapolation, but more importantly, in the correcting amplitudes and retrieving sediment-related internal multiples in the downgoing transmitted field. This transmitted field simply cannot be obtained by conventional wavefield extrapolation.

Although better than conventional extrapolation, the quality of fields estimated by the Marchenko scheme in highly complex media suffers from the assumptions made in the key components of the current scheme. When using the complex migration velocity model with sharp salt boundaries, using the time-reversed transmitted fields in that model as an estimate of the initial focusing function leads to errors in the final estimate. That is because, unlike the case of simpler media, in a complex subsalt model the time-reversed fields are poor approximations to the inverse transmission response required for the initial focusing function. In addition, the relatively simple time windowing approach used in the current separation scheme may not be ideal in such highly complex media: while it indeed satisfies causality of the redatumed fields, it may well fail to capture all of the necessary contributions to the focussing function that may occur at later times. We point that improving the estimate of the initial focusing function, and choosing more suitable separation filters may help in improving Marchenko redatuming in highly complex media.

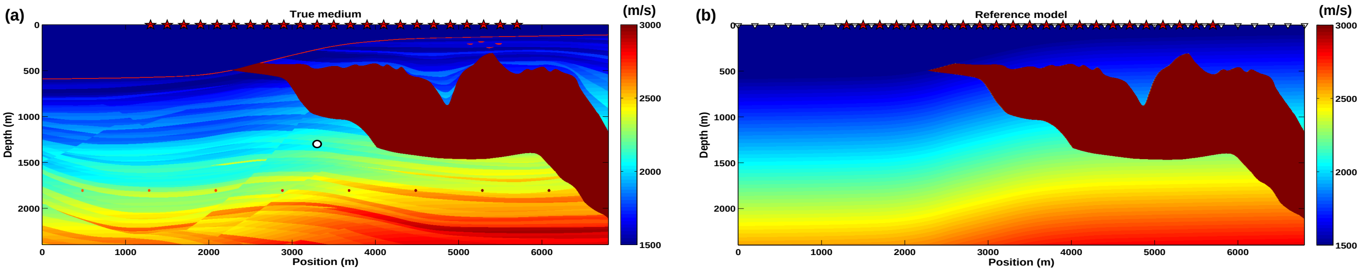

Figure 2: Sigsbee wavespeed model used for Marchenko redatuming tests. Panel (a) shows the “true” model where physical propagation occurs. In (a), the white dot indicates the location where we wish to reconstruct the subsurface wavefield. Panel (b) is the reference model used both for conventional reverse-time extrapolation and for Marchenko redatuming. The red stars and white triangles at the top of the models indicate, respectively, where the sources and receivers for the reflection data are placed.

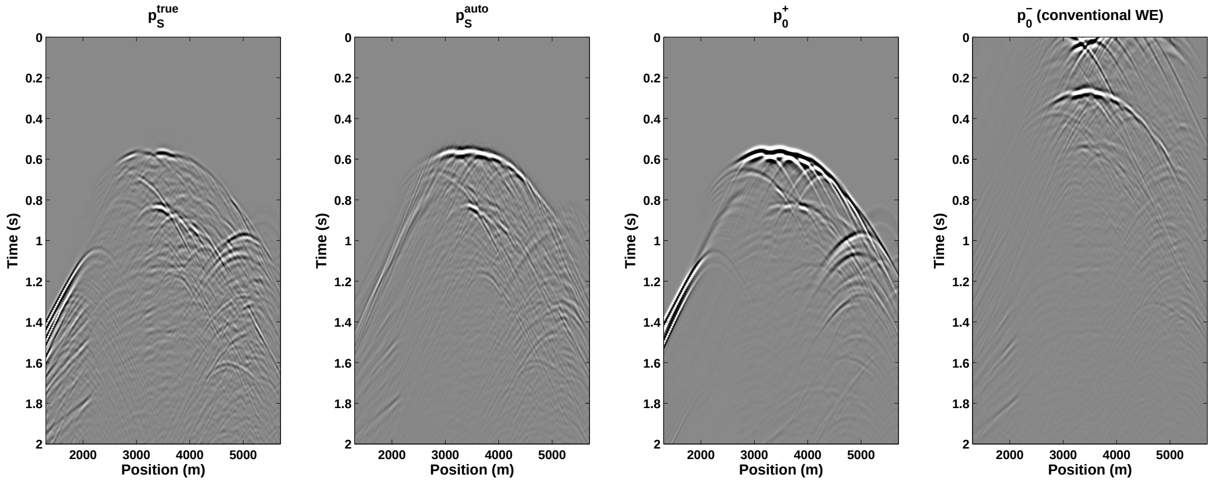

Figure 3: Forward modeled and redatumed fields from the Sigsbee example. Here, the field p_0^+ is the reference forward-modeled pressure field between the focusing point and the surface of the model in Figure 2b. The field p_S^{true} is the forward-modeled field from the focusing point to the surface in the true model in Figure 2a, minus the field p_0^+. The field p_0^- is the result of conventional reverse-time extrapolation of the reflection data, using the model in Figure 2b. Finally, p_S^{auto} is the redatumed scattered field estimated by Marchenko autofocusing, using p_0^+ as the reference field for the iterative procedure.

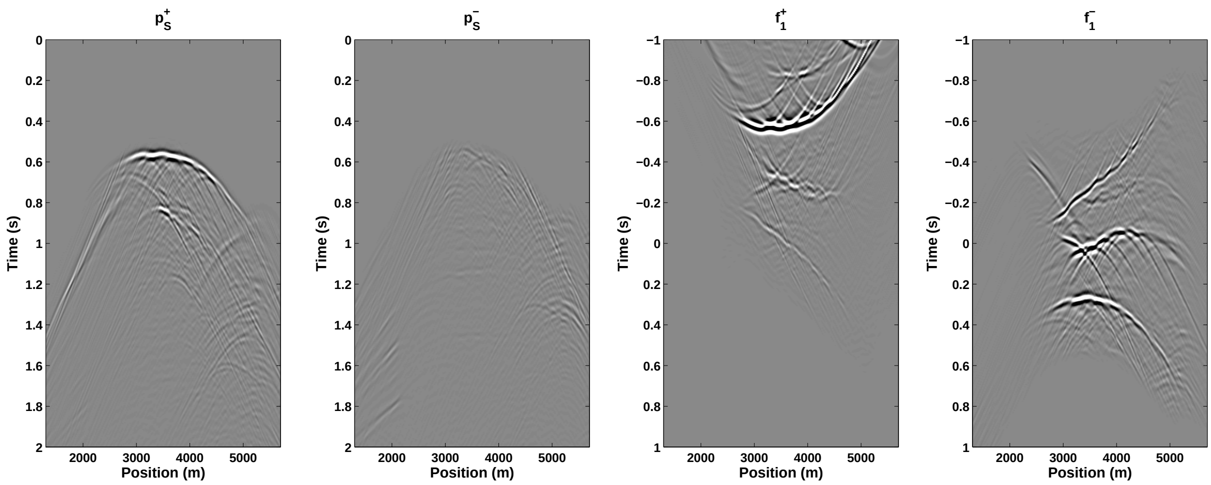

Figure 4: Redatumed fields resulting from three iterations of Marchenko autofocusing. The fields p_S^+ and p_S^- are, respectively, the down- and upgoing components of p_S^{auto} in Figure 3. Likewise, f_1^+ and f_1^- are the down- and upgoing components of the f_1 focusing function in equations 1 through 5.

REFERENCES

Behura, J., K. Wapenaar, and R. Snieder, 2012, Newton-Marchenko-Rose Imaging: SEG Technical Program Expanded Abstracts, 1–6.

Broggini, F., R. Snieder, and K. Wapenaar, 2011, Connection of scattering principles: Focusing the wavefield without source or receiver: 81st Annual International Meeting, SEG, Expanded Abstracts, **30**, 3845–3850.

———, 2012, Focusing the wavefield inside an unknown 1d medium: Beyond seismic interferometry: Geophysics, **77**, A25–A28.

Broggini, F., K. Wapenaar, J. van der Neut, and R. Snieder, 2014, Data-driven green's function retrieval and application to imaging with multidimensional deconvolution: Journal of Geophysical Research: Solid Earth, **119**, 425–441.

Ravasi, M., I. Vasconcelos, and A. Curtis, 2014, Beyond conventional migration: nonlinear subsalt imaging with transmissions and two-sided illumination: Presented at the 76th EAGE Conference & Exhibition Extended Abstracts.

van der Neut, J., E. Slob, K. Wapenaar, J. Thorbecke, R. Snieder, and F. Broggini, 2013, Interferometric redatuming of autofocused primaries and internal multiples: SEG Technical Program Expanded Abstracts, 4589–4594.

van der Neut, J., I. Vasconcelos, and K. Wapenaar, 2014, An Interferometric Interpretation of Marchenko Redatuming: Presented at the 76th EAGE Conference & Exhibition Extended Abstracts.

van Manen, D.-J., J. O. A. Robertsson, and A. Curtis, 2007, Exact wave field simulation for finite-volume scattering problems: The Journal of the Acoustical Society of America, **122**.

Vasconcelos, I., 2013, Source-receiver, reverse-time imaging of dual-source, vector-acoustic seismic data: Geophysics, **78**, WA123–WA145.

Vasconcelos, I., M. Ravasi, and J. van der Neut, 2014, An interferometry-based, subsurface-domain objective function for targeted waveform inversion: Presented at the 76th EAGE Conference & Exhibition Extended Abstracts.

Vasconcelos, I. and J. Rickett, 2013, Broadband extended images by joint inversion of multiple blended wavefields: Geophysics, **78**, WA147–WA158.

Wapenaar, K., F. Broggini, E. Slob, and R. Snieder, 2013a, Three-dimensional single-sided marchenko inverse scattering, data-driven focusing, green's function retrieval, and their mutual relations: Phys. Rev. Lett., **110**, no. 8, 084301.

Wapenaar, K., E. Slob, J. Neut, J. Thorbecke, F. Broggini, and R. Snieder, 2013b, Three-dimensional marchenko equation for green's function retrieval beyond seismic interferometry: SEG Technical Program Expanded Abstracts, 4573–4578.

Wapenaar, K., J. Thorbecke, J. van der Neut, I. Vasconcelos, and E. Slob, 2014, Marchenko imaging below an overburden with random scatterers: Presented at the 76th EAGE Conference & Exhibition Extended Abstracts.